Comprehensive Analyses of Data Collected from TEREK (Solar EUV Telescope) RES-C (Solar X-Ray Spectrometer) and SORS (Solar Radio Spectrometer) on board CORONAS-I Using Magnetohydrodynamic Models

FINAL REPORT
Award Number: NAGW-4665
Period of Performance: June 1, 1995 - November 30, 1996

Prepared by:

S. T. Wu
Distinguished Professor, University of Alabama System
Department of Mechanical and Aerospace Engineering
Director, Center for Space Plasma and Aeronomic Research
The University of Alabama in Huntsville
Huntsville, AL 35899
(205) 890-6413 wus@cspar.uah.edu

In this grant (NAGW-4665) our achievements will be summarized into three categories as follows:

I. Visit of Co-Investigators

The Co-Investigators, Drs. Vladimir Obridko, IZMIRAN, SORS, Russia, Victor Fomichev, IZMIRAN, Russia and Dr. Vladimir Slemzin visited the facilities at The University of Alabama in Huntsville during October/November 1995. They gave several seminars during their stay at the Center for Space Plasma and Aeronomic Research including: "Solar XUV-imaging spectroscopy with the TEREK telescope and RES Spectroheliometer on-board the CORONAS-I Satellite" and "The role of solar magnetic field in the neutrino flux modulation" and "'System' Space Mission for Solar Investigation". Scientist from NASA/MSFC/SSL, faculty members and graduate students from UAH attended and participated in the discussions at these seminars.

Two events observed by CORONAS-I and YOHKOH were selected for coronal hole analysis. These images were stored into the CSPAR computer with the corresponding magnetic field measurements obtained by Stanford University. Construction of a 3-D global potential magnetic field to simulate the observed features of CORONAS-I up to distances of 4 R_s was accomplished. Results were presented at the SCOSTEP/STEP Workshop WG-1 Workshop on Measurements and Analyses of the 3-D Solar Magnetic Field" held April 9 - 11, 1996, at Huntsville, Alabama, USA.

II. Presentations

Three presentations at international meeting were made. These presentations are:

- Analyses and Modeling of Coronal Holes Observed by CORONAS-I I. Morphology and Magnetic Field Configuration, V. Obridko, V. Fomichev, A. F. Kharshiladze, V. Slemzin, S. T. Wu, J. Ding, and D. Hathaway, Presentation "SCOSTEP/STEP Workshop WG-1 Workshop on Measurements and Analyses of the 3-D Solar Magnetic Field" held April 9 - 11, 1996, at Huntsville, Alabama, USA.

- Analyses and Modeling of Coronal Holes Observed by CORONAS-I: II. MHD Simulation, A. H. Wang, S. T. Wu, D. Hathaway, M. Dryer, V. Obridko, V. Forichev, A. F. Kharshiladze, L. Zhitnik and V. Slemzin, Present at the SOLTIP III Symposium in Beijing China, October 14-18, 1996, *Chinese Journal of Space Science in English*, 1997, (in press)

- An Alternative Progressive-Extension-Method (PEM) for Extrapolation of Non-linear Force Free Field (NLFF) Using Vector Magnetograms, M. T. Song, and S. T. Wu, Presentation "SCOSTEP/STEP Workshop WG-1 Workshop on Measurements and Analyses of the 3-D Solar Magnetic Field" held April 9 - 11, 1996, at Huntsville, Alabama, USA.

- Indirect Evidence for the 3-D Magnetic Configuration from SOHO UVCS Observations Poletto, S. T. Suess, A.-H. Wang, and S. T. Wu, Presentation "SCOSTEP/STEP Workshop WG-1 Workshop on Measurements and Analyses of the 3-D Solar Magnetic Field" held April 9 - 11, 1996, at Huntsville, Alabama, USA.

III. Papers Published, Accepted, And Submitted For Publication In Journals

Six manuscripts have been published, accepted or submitted for publication in journals. These manuscripts are:

- Analyses and Modeling of Coronal Holes Observed by CORONAS-I I. Morphology and Magnetic Field Configuration, V. Obridko, V. Fomichev, A. F. Kharshiladze, V. Slemzin, S. T. Wu, J. Ding, and D. Hathaway, to be submitted to *Solar Physics*, (in preparation).

- Analyses and Modeling of Coronal Holes Observed by CORONAS-I: II. MHD Simulation, A. H. Wang, S. T. Wu, D. Hathaway, M. Dryer, V. Obridko, V. Forichev, A. F. Kharshiladze, L. Zhitnik and V. Slemzin, Present at the SOLTIP III Symposium in Beijing China, October 14-18, 1996, *Chinese Journal of Space Science in English*, 1997, (in press).

- Disruption of Helmet Streamers by Current Emergence, W. P. Guo, S. T. Wu, and E. Tandberg-Hanssen, *The Astrophysical Journal*, **469**, 944-951, 1996

- Dynamics Evolution of a Coronal Streamer-Flux Rope System. II. A Self-Consistent Non-Planar Magnetohydrodynamic Simulation, S. T. Wu, W. P. Guo and M. Dryer, *Solar Physics*, 1996 (in press).

- A Self-Consistent Numerical Magnetohydrodynamics (MHD) Model of Helmet Streamers and Flux-Rope Interactions: Initiations and Propagation of Coronal Mass Ejections (CMEs) S. T. Wu and W. P. Guo, Proceeding of the Chapman Conference on Coronal Mass Ejections, Bozeman, Montana, August 11-15, 1996, in Coronal Mass Ejections: Causes and Consequences, (N. Crooker, J. Joslyn, J. Feynman, eds.), 1996 (in press)

- Inferences on Coronal Magnetic Fields from SOHO UVCS Observations, G. Poletto M. Romoli, S. T. Suess, A. H. Wang, S. T. Wu, Proceedings of the "SCOSTEP/STEP Workshop WG-1 Workshop on Measurements and Analyses of the 3-D Solar Magnetic Field" held April 9 - 11, 1996, at Huntsville, Alabama, USA *Special Issue of Solar Physics*, 1996 (in press).

The manuscripts of these papers are included in the Appendix.

Analyses And Modeling Of Coronal Holes Observed By Coronas-I: II. MHD Simulation

A. H. Wang and S. T. Wu
CSPAR, Univ. of Alabama in Huntsville, AL 35899, USA

D. Hathaway
SSL NASA/MSFC, Huntsville, AL 35812, USA

Murray Dryer
NOAA/SEC, Boulder, CO 80303, USA

V. Obridko, V. Fomichev and A. F. Kharshiladze
IZMIRAN Institute, Russia

L. Zhitnik and V. Slenzin
P. N. Ledebev Physics Institute, Russia

Nov. 13, 1996

ABSTRACT

By using the observed magnetic field data obtained from the Wilcox Solar Observatory at Stanford University as the inputs to a two-dimensional plane-of-sky magnetohydrodynamic model, via numerical relaxation method, we have deduced the plasma and magnetic field parameters for the observed coronal hole by CORONAS-I on June 17, 1994. The method for this self-consistent MHD analysis will be discussed in detail. Numerical results for the magnetic field configuration, velocity distribution, density and temperature distributions will be presented. We have converted the computed density to polarization brightness in order to directly compare the MHD outputs with observations.

1 Introduction

In the paper I, two low-latitude coronal holes observed by CORONAS-I on April 30 and June 17 in 1994 are analyzed with magnetic field measurements obtained by Stanford University and Kitts Peak solar observatories. The three dimensional potential magnetic field lines based on the observed photospheric magnetic vector were extrapolated to 2 solar radii by source surface model and after 2 solar radii all the field lines are assumed to be radial. Also we don't have any information about the plasma parameters.

In this paper, we introduced a self-consistent MHD theory to reveal the plasma parameters, such as density, temperature and velocity distribution, and more realistic magnetic field. We have chosen the potential magnetic field configuration based on the observation magnetic vector on June 17, 1994 from the paper I as the initial magnetic field lines and add the density, temperature and velocity. Using the numerical relaxation method to get the quasi-steady state of MHD coronal structure. In section II we will give detailed description of the mathematic model. In section III the numerical simulation results including magnetic field configuration, plasma density, temperature and velocity will be shown and discussed. Also the radial velocity will be compared with the observed solar wind speed on Jun 17, 1994.

2 Mathematic Theory

To demonstrate this method we have simplified the three dimensional MHD to a two dimensional MHD. The governing equations for two dimensional, time dependent, a single fluid, fully ionized plasma with volumetric heating and thermal conduction in spherical coordinates can be written as follows :

$$\frac{\partial \rho}{\partial t} = -\frac{1}{r^2}\frac{\partial (r^2 \rho v_r)}{\partial r} - \frac{1}{r sin\theta}\frac{\partial (\rho v_\theta sin\theta)}{\partial \theta} \tag{1}$$

$$\frac{\partial v_r}{\partial t} = -v_r\frac{\partial v_r}{\partial r} - \frac{v_\theta}{r}\frac{\partial v_r}{\partial \theta} - \frac{1}{\rho}[\frac{\partial (\rho RT)}{\partial r} + \frac{{B_\theta}^2}{r} + B_\theta(\frac{\partial B_\theta}{\partial r} - \frac{1}{r}\frac{\partial B_r}{\partial \theta})] + \frac{v_\theta^2}{r} - g(r) \tag{2}$$

$$\frac{\partial v_\theta}{\partial t} = -v_r\frac{\partial v_\theta}{\partial r} - \frac{v_\theta}{r}\frac{\partial v_\theta}{\partial \theta} - \frac{1}{\rho}[\frac{\partial (\rho RT)}{r\partial \theta} - \frac{B_r B_\theta}{\rho r} - B_r(\frac{\partial B_\theta}{\partial r} - \frac{1}{r}\frac{\partial B_r}{\partial \theta})] - \frac{v_r v_\theta}{r} \tag{3}$$

$$\frac{\partial B_r}{\partial t} = \frac{1}{r sin\theta}\frac{\partial}{\partial \theta}[sin\theta(v_r B_\theta - v_\theta B_r)] \quad (4)$$

$$\frac{\partial B_\theta}{\partial t} = -\frac{1}{r}\frac{\partial}{\partial r}[r(v_r B_\theta - v_\theta B_r)] \quad (5)$$

$$\begin{aligned}\frac{\partial T}{\partial t} &= -(\gamma-1)[\frac{1}{r^2}\frac{\partial(r^2 v_r)}{\partial r} + \frac{1}{r sin\theta}\frac{\partial(v_\theta sin\theta)}{\partial \theta}]T \\ &- v_r\frac{\partial T}{\partial r} - \frac{v_\theta}{r}\frac{\partial T}{\partial \theta} + q_e(r) - \frac{1}{\rho C_v}[\frac{1}{r^2}\frac{\partial(r^2 q_r)}{\partial r} \\ &+ \frac{1}{r sin\theta}\frac{\partial(q_\theta sin\theta)}{\partial \theta}] \quad (6)\end{aligned}$$

$$p = \rho R T \quad (7)$$

where ρ is the plasma density ($\rho = n m_p$); T is the temperature; p is the isotropic pressure; v_r and v_θ are the flow velocities in the radial direction and meridional direction, respectively; B_r and B_θ are magnetic field intensities in the radial direction and meridional direction, respectively. C_v is the specific heat at constant volume for a monoatomic gas, γ (adiabatic index) is 5/3, and g is the gravitational acceleration. $q_e(r)$ is the volumetric heat source, given by

$$q_e(r) = C e^{-0.1(r-R_\odot)/R_\odot} \quad (8)$$

where $R_\odot$ is the solar radius, C is arbitrary constant. As in Suess, Wang and Wu (1996) and Steinolfson (1988), the purpose of adding the heating term is to obtain a thin current sheet in the streamer region and the adiabatic index could be 5/3. q_r and q_θ are the radial and meridional thermal conductive fluxes for a Lorentz gas, given by

$$\nabla \cdot \mathbf{q} = \nabla \cdot [\kappa_{||} T^{5/2}(\mathbf{B}\cdot\nabla\mathbf{T})\frac{\mathbf{B}}{\mathbf{B^2}}] \quad (9)$$

B is the magnetic field vector and $\kappa_{||}$ is the collisional thermal conductivity along the magnetic field lines as given by Spitzer (1962). Thermal conduction slightly reduces the heat accumulation rate in the streamer region [see Suess, Wang and Wu (1996)].

The computational domain is in a meridional plane from the north pole to the south pole in the θ direction, i.e. 0° to 180° and from the solar surface about $1.5R_\odot$ to $7R_\odot$ in the radial direction. The bottom boundary is a physical boundary we used self-consistent characteristic method to determine the physical parameters. At the top boundary since the flow is super-sonic and super-Alfvenic, a linear extrapolation method has been used. At two side

boundary, i.e. at north pole and south pole, the symetric boundary conditions assumed. The numerical scheme we used is the fully implicit, continuous Eulerian scheme (FICE) which was developed by Hu and Wu (1984). The detail boundary conditions and numerical scheme are described by Wang et al. (1995) and Suess, Wang and Wu (1996).

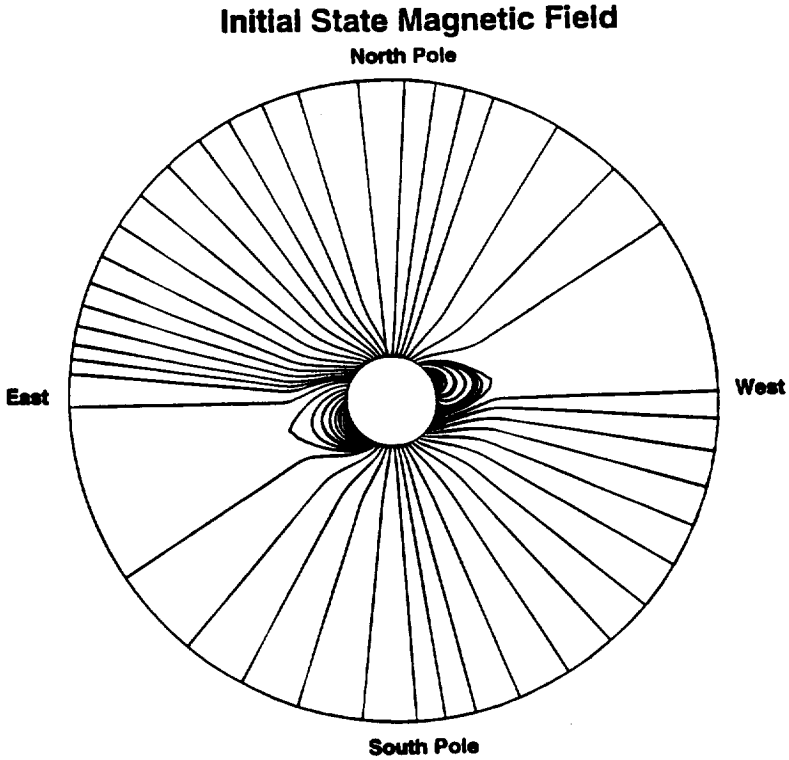

Figure 1: The right half plane is at $\phi = 352.5°$ and the left half plane is at $\phi = 172.5°$.

To initiate the numerical calculation, we choose an initial trial state of a extrapolated potential magnetic field based on the observation data by Stanford University on June 17, 1994 at $\phi = 172.5°$ and $\phi = 352.5°$ which are from the paper I. At $\phi = 172.5°$ and $\phi = 352.5°$ the magnitude of B_ϕ compared with B_r and B_θ are very small and the ratio of $B_\phi/(B_r, B_\theta)$ is about 0.01. Figure 1. shows the field configuration. In this initial state, density and effective temperature are assumed dependent on radius and latitude. At the closed magnetic field lines region density is high than at the open field lines regions. The maximum value of number density is $2.02 \times 10^8 cm^{-3}$ and the minimum value is $0.88 \times 10^8 cm^{-3}$. To get high velocity at the open field region

the effective temperature is assumed higher than at the closed field region. The maximum value is 1.92×10^6 degree and the minimum value is 1.77×10^6 degree. The velocity distribution is arbitrary, but along the magnetic field.

3 Numerical Simulation Results

In this section the numerical simulation results including magnetic field configuration, density, temperature and velocity will be shown. Fig. 2 is the magnetic field lines. Fig. 3 shows the density, effective temperature and radial velocity distributions vs latitudial angle at several distances.

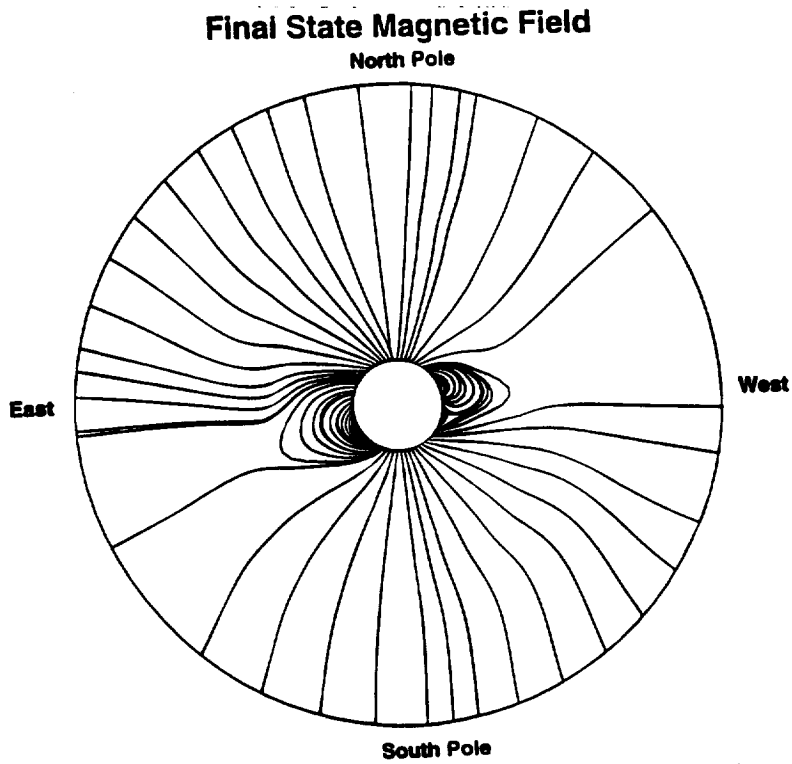

Figure 2: The relaxation quasi-steady state. The right half plane is at $\phi = 352.5°$ and the left half plane is at $\phi = 172.5°$.

Comparing Fig. 2 with Fig. 1 the magnetic field configuration changes a little bit because the velocity in this case is small. From Fig. 3 it is obvious at two closed magnetic field lines regions the densities are high and the velocities are low. At the open magnetic field lines regions the densities are low and the velocities are high. The acceleration at the open magnetic field regions in this

case are due to high effective temperatures. This effect is shown on Fig. 3 and the higher speed regions are correspond with the higher effective regions.

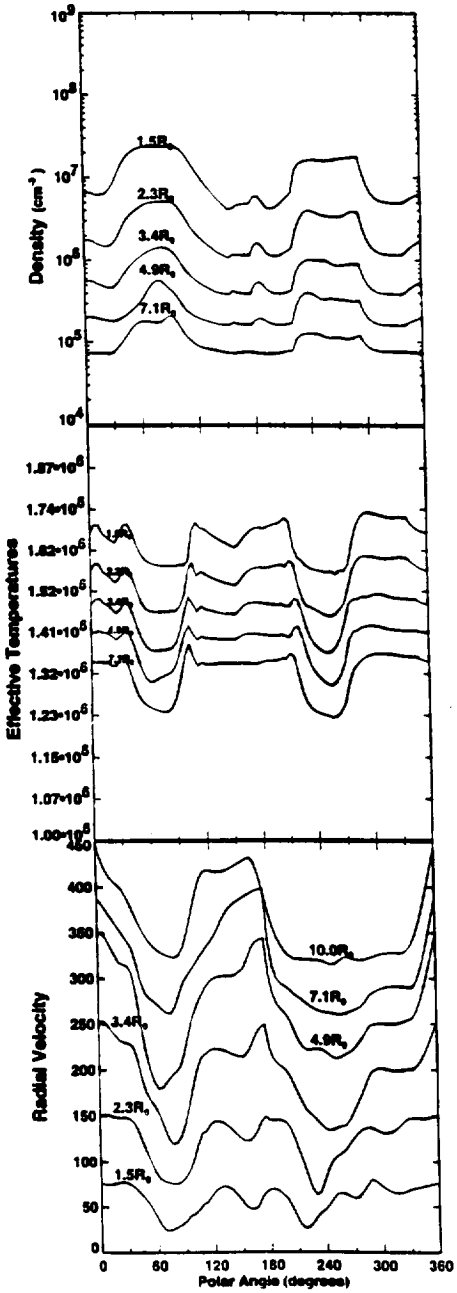

Figure 3: Density, effective temperature and radial velocity variations with polar angle at several different radii. 0^o and 360^o represent the north pole and south pole, respectively.

To comparing our numerical simulation velocity with the observed solar wind speed on the same day Fig. 4 shows the solar wind speed during the

flight of the CORONAS-I satellite from March 12 to July 5, 1994. At the day of June 17, 1994 the solar wind speed is about $450 km/sec$ and in our numerical simulation the radial velocity at $7.1 R_\odot$ is about this value.

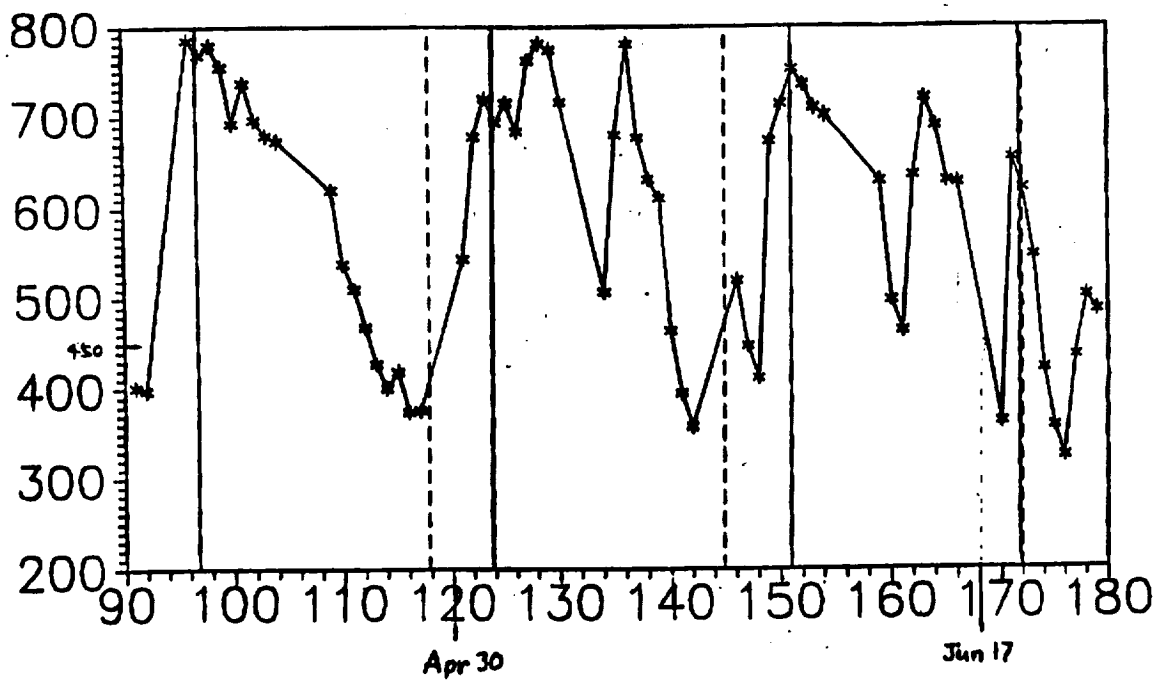

Figure 4: Solar Wind IMP8 velocities. Abscissa is the number of the day in 1994. The velocity unit is KM/SEC.

4 Summary

- A method based on the self-consistent MHD theory to reveal the plasma parameters and fields (magnetic and velocity) for a observed global coronal features in the plane of sky which include the streamers and holes is presented.
- The next step for our future study is extented current development to a full three-dimensional configuration.

Reference

Hu, Y. Q. and S. T. Wu: J. Computational Phys., 55, 33, 1984

Spitzer, L., Physics of Fully Ionized Gases. 2nd rev. ed., John Wiley, New York, 1962

Suess, S. T., A. H. Wang and S. T. Wu: J. Geophys. Res., 101, 19957, 1996

Obridko, V., V. Fomichev, A. F. Kharshiladze, I. Zhitnik, V. Slemzin, S. T. Wu, J. Ding and D. Hathaway: paper I

Wang, A. H., S. T. Wu, S. T. Suess and G. Poletto: Sol. Phys., 161, 365, 1995